

1 **Transmission of one predicts another: Apathogenic proxies for transmission dynamics**
2 **of a fatal virus**

3
4 Marie L.J. Gilbertson^{1†}, Nicholas M. Fountain-Jones^{2*}, Jennifer L. Malmberg^{3,4*}, Roderick B.
5 Gagne^{3,5}, Justin S. Lee³, Simona Kraberger⁶, Sarah Kechejian³, Raegan Petch³, Elliott Chiu³,
6 Dave Onorato⁷, Mark W. Cunningham⁸, Kevin R. Crooks⁹, W. Chris Funk¹⁰, Scott Carver², Sue
7 VandeWoude³, Kimberly VanderWaal¹, Meggan E. Craft^{1,11}

8 †Corresponding author: jone1354@umn.edu

9 *These authors contributed equally

10 ¹Department of Veterinary Population Medicine, University of Minnesota, St Paul, MN 55108.

11 ²School of Natural Sciences, University of Tasmania, Hobart Australia 7001.

12 ³Department of Microbiology, Immunology, and Pathology, Colorado State University, Fort
13 Collins, CO 80523

14 ⁴Department of Veterinary Sciences, University of Wyoming, Laramie, Wyoming 82071.

15 ⁵Wildlife Futures Program, Department of Pathobiology, University of Pennsylvania,
16 Philadelphia, PA 19104

17 ⁶The Biodesign Center for Fundamental and Applied Microbiomics, Arizona State University,
18 Tempe, Arizona, AZ 85287, USA

19 ⁷Fish and Wildlife Research Institute, Florida Fish and Wildlife Conservation Commission,
20 Naples, FL 34114.

21 ⁸Fish and Wildlife Research Institute, Florida Fish and Wildlife Conservation Commission,
22 Gainesville, FL 32601.

23 ⁹Department of Fish, Wildlife, and Conservation Biology, Colorado State University, Fort Collins,
24 CO 80523.

25 ¹⁰Department of Biology, Graduate Degree Program in Ecology, Colorado State University, Fort
26 Collins, CO 80523.

27 ¹¹ Department of Ecology, Evolution and Behavior, University of Minnesota, St Paul, MN 55108.

28

29 **Classification**

30 Biological Sciences: Ecology

31

32 **Keywords**

33 transmission tree; exponential random graph model; network modeling; disease model; Florida
34 panther

35

36 **Abstract**

37 Identifying drivers of transmission prior to an epidemic—especially of an emerging pathogen—is
38 a formidable challenge for proactive disease management efforts. To overcome this gap, we
39 tested a novel approach hypothesizing that an apathogenic virus could elucidate drivers of
40 transmission processes, and thereby predict transmission dynamics of an analogously
41 transmitted virulent pathogen. We evaluated this hypothesis in a model system, the Florida
42 panther (*Puma concolor coryi*), using apathogenic feline immunodeficiency virus (FIV) to predict
43 transmission dynamics for another retrovirus, pathogenic feline leukemia virus (FeLV). We
44 derived a transmission network using FIV whole genome sequences, and used exponential
45 random graph models to determine drivers structuring this network. We used the identified
46 drivers to predict transmission pathways among panthers; simulated FeLV transmission using
47 these pathways and three alternate modeling approaches; and compared predictions against
48 empirical data collected during a historical FeLV outbreak in panthers. FIV transmission was
49 primarily driven by panther age class and distances between panther home range centroids.
50 Prospective FIV-based predictions of FeLV transmission dynamics performed at least as well as
51 simpler, often retrospective approaches, with evidence that FIV-based predictions could capture
52 the spatial structuring of the observed FeLV outbreak. Our finding that an apathogenic agent

53 can predict transmission of an analogously transmitted pathogen is an innovative approach that
54 warrants testing in other host-pathogen systems to determine generalizability. Use of such
55 apathogenic agents holds promise for improving predictions of pathogen transmission in novel
56 host populations, and can thereby revolutionize proactive pathogen management in human and
57 animal systems.

58

59 **Significance Statement**

60 Predicting infectious disease transmission dynamics is fraught with assumptions which limit our
61 ability to proactively develop targeted control strategies. We show that transmission of non-
62 disease causing (apathogenic) agents provides invaluable insight into drivers of transmission
63 prior to outbreaks of more serious diseases. Integrating genomic and network approaches, we
64 tested an apathogenic virus as a proxy for predicting transmission dynamics of a deadly virus in
65 the Florida panther. We found that apathogenic virus-based predictions of pathogen
66 transmission dynamics performed at least as well as simpler transmission models, and offered
67 the advantage of prospectively identifying the underlying management-relevant drivers of
68 transmission. Our innovative approach offers an opportunity to proactively design disease
69 control strategies in at-risk animal and human populations.

70

71

72

73 **Introduction**

74 Infectious disease outbreaks can have profound impacts on conservation, food security,
75 and global health and economics. Mathematical models have proven a vital tool for
76 understanding transmission dynamics of pathogens (1, 2), but struggle to predict the dynamics
77 of novel or emerging agents (3, 4). This is at least partially due to the challenges associated
78 with characterizing contacts relevant to transmission processes. Common modeling approaches
79 that assume all hosts interact and transmit infections to the same degree ignore key drivers of
80 transmission. Such drivers can include specific transmission-relevant behaviors including
81 grooming or fighting in animals (5), concurrent sexual partnerships in humans (6), or assortative
82 mixing (7), and result in flawed epidemic predictions (8, 9). Further, identifying drivers of
83 transmission and consequent control strategies for any given pathogen is typically done
84 reactively or retrospectively in an effort to stop or prevent further outbreaks or spatial spread
85 (e.g. 10–12). These constraints limit the ability to perform prospective disease management
86 planning tailored to a given target population, increasing the risk of potentially catastrophic
87 pathogen outbreaks, as observed in humans (13–15), domestic animals (16, 17), and species of
88 conservation concern including Ethiopian wolves (18), African lions (19), black-footed ferrets
89 (20), and Florida panthers (21).

90 A handful of studies have evaluated whether common infectious agents present in the
91 healthy animal microbiome or virome can indicate contacts between individuals that may
92 translate to interactions promoting pathogen transmission. Such an approach circumvents some
93 of the uncertainties associated with more traditional approaches to contact detection (8). In
94 these cases, genetic evidence from the transmissible agent itself is used to define between-
95 individual interactions for which contact was sufficient for transmission to occur. Results of such
96 studies show mixed success (22–27). For example, members of the same household have been
97 found to share microbiota (28, 29), but disentangling social mechanisms of this sharing is
98 complicated by shared diets, environments, behaviors, etc. (30). In animals, studies of

99 *Escherichia coli* in Verreaux's sifaka and giraffe have found strain sharing relationships to be
100 tied to social interactions (22, 23), but the same was not found in a similar study of elephants
101 (26).

102 These studies have, however, revealed ideal characteristics of non-disease inducing
103 infectious agents (hereafter, *apathogenic agents*) for use as markers of transmission-relevant
104 interactions. Such apathogenic agents should have rapid mutation rates to facilitate discernment
105 of transmission relationships between individuals over time (31, 32). Furthermore, these agents
106 should be relatively common and well-sampled in a target population, have a well-characterized
107 mode of transmission, and feature high strain alpha-diversity (local diversity) and high strain
108 turnover (32, 33). RNA viruses align well with these characteristics (34, 35) such that
109 apathogenic RNA viruses could act as "proxies" of specific modes of transmission (i.e., direct
110 transmission) and indicate which drivers underlie transmission processes (36). Such drivers,
111 including but not limited to host demographics, relatedness, specific behaviors, or space use,
112 would subsequently allow prediction of transmission dynamics of pathogenic agents with the
113 same mode of transmission (32).

114 Here, we test the feasibility of this approach using a naturally occurring host-pathogen
115 system to test if an apathogenic RNA virus can act as a proxy for direct transmission processes
116 and subsequently predict transmission of a pathogenic RNA virus. Florida panthers (*Puma*
117 *concolor coryi*) are an endangered subspecies of puma found only in southern Florida and have
118 been extensively studied and monitored for almost four decades. We have documented that this
119 population is infected by several feline retroviruses relevant to our study questions. Feline
120 immunodeficiency virus (FIVpco; hereafter, FIV) occurs in approximately 50% of the population
121 and does not appear to cause significant clinical disease (37). FIV is transmitted by close
122 contact (i.e., fighting and biting), generally has a rapid mutation rate (intra-individual evolution
123 rate of 0.00129 substitutions/site/year; 38), and, as a chronic retrovirus infection, can be
124 persistently detected after the time of infection. Panthers are also affected by feline leukemia

125 virus (FeLV), also a retrovirus, which spills over into their population following exposure of
126 panthers to infected domestic cats (39). Once spillover occurs, FeLV is transmitted between
127 panthers by close contact and results in progressive, regressive, or abortive infection states
128 (21). Progressive cases are infectious and result in mortality; regressive infections are not
129 expected to be infectious—though this is unclear in panthers—and recover (21, 40, 41).
130 Abortive cases clear infection and are not themselves infectious (41). A high mortality FeLV
131 outbreak was documented among panthers in 2002-2004 and has been characterized in several
132 studies (21, 39, 42).

133 This well-observed historical outbreak is a key advantage of this naturally-occurring
134 system, allowing us to compare our predictions against empirical observations. The objectives
135 of this study were therefore: (1) to determine which factors shape FIV transmission in Florida
136 panthers, and (2) test if these factors can predict transmission dynamics of analogously-
137 transmitted FeLV in panthers. Success of this approach in our model system would pave the
138 way for testing similar apathogenic agents in other host-pathogen systems, thereby improving
139 our ability to predict transmission dynamics of novel agents in human and animal populations.

140

141 **Methods**

142 *Dataset assembly*

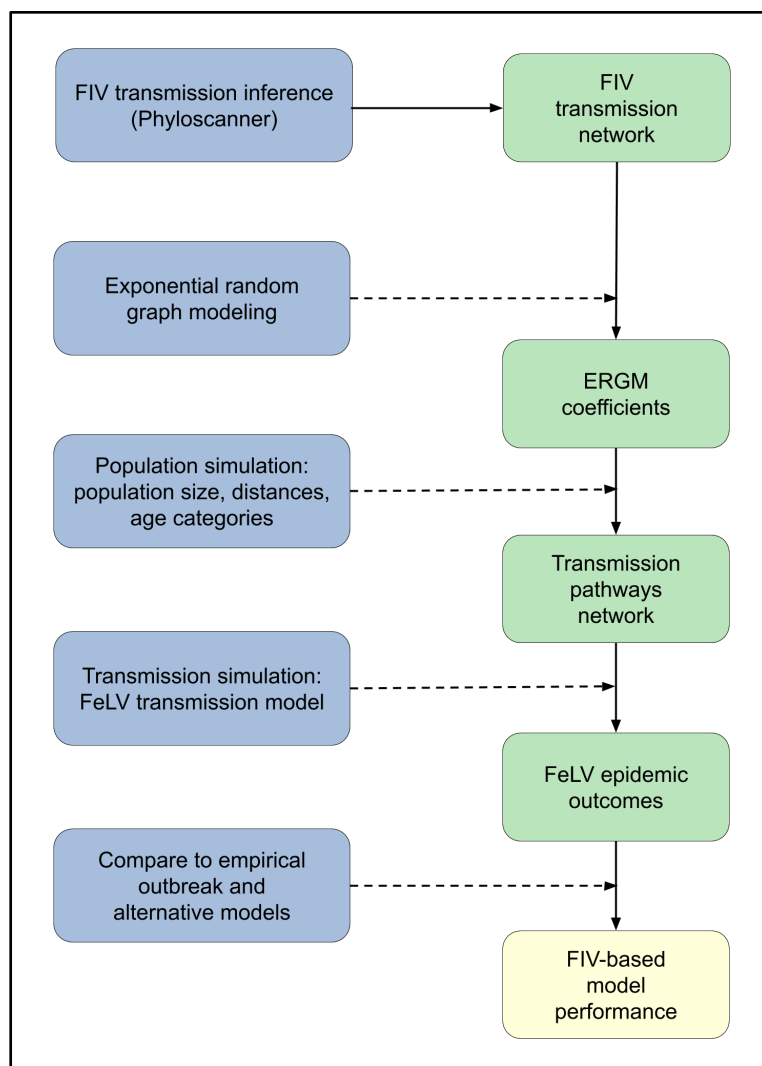
143 We assembled an extensive dataset covering almost 40 years of Florida panther
144 research. Ongoing panther management has documented age and sex of monitored panthers.
145 In addition, a subset of the population is monitored using very high frequency (VHF) telemetry
146 collars, with relocations determined via aircraft typically three times per week. Previous panther
147 research has generated a microsatellite dataset for monitored panthers (43), and a dataset of
148 60 full FIV genomes (proviral DNA sequenced within a tiled amplicon framework in 44). In
149 addition, the historical FeLV outbreak in panthers was well documented (21, 39), providing key
150 observations regarding FeLV dynamics in free-ranging panthers. To augment these

151 observations, we also used an FeLV database which documents FeLV status (positive and
152 negative) for 31 panthers as determined by qPCR from 2002-04.

153

154 *FIV transmission inference*

155 To determine drivers of FIV transmission, we first generated a “who transmitted to
156 whom” transmission network using 60 panther FIV genomes collected from 1988 to 2011 (see
157 Figure 1 for workflow across all analyses). We used the program PhyloScanner (45), which
158 maximizes the information gleaned from next generation sequencing reads to infer transmission
159 relationships. PhyloScanner operates in a two step process, first inferring within- and between-
160 host phylogenies in windows along the FIV genome, and then analysing those phylogenies to
161 produce transmission trees or networks. For step one, we used 150bp windows, allowing 25bp
162 overlap between windows. To test sensitivity to this choice, we separately ran a full
163 PhyloScanner analysis with 150bp windows, but without overlap between windows
164 (supplementary methods). For step two, we held k , which penalizes within-host diversity, equal
165 to 0. We used a patristic distance threshold of 0.05 and allowed missing and more complex
166 transmission relationships. Because we had uneven read depth across FIV genomes, we
167 downsampled to a maximum of 200 reads per host. The output of the full PhyloScanner analysis
168 was a single transmission network (hereafter, *main FIV network*), but see supplementary
169 methods for details regarding analysis of the sensitivity of our results to variations in and
170 summary across multiple transmission networks (resulting in two *summary FIV networks*).



171
172 **Figure 1:** Conceptual workflow across all analysis steps. Processes are shown on the left in
173 blue; specific outcomes are shown on the right in green; the final analysis outcome is in yellow
174 at the bottom right. Solid lines show direct flows or outcomes. Dashed lines show processes
175 acting on or in concert with prior outcomes: for example, exponential random graph modeling
176 (ERGM) was performed using the FIV transmission network, and the combination of the two
177 produced the ERGM coefficients outcome.
178
179 *Statistical analysis of FIV transmission networks*

180 We performed statistical analysis of unweighted, binary FIV transmission networks using
181 exponential random graph models (ERGMs), which account for non-independence in network
182 structure (46). The network structural terms we considered included an intercept-like edges term
183 (46), geometrically weighted edgewise shared partner distribution (*gwesp*; representation of
184 network triangles), alternating k-stars (*altkstar*; representation of star structures), and 2-paths (2
185 step paths from i to k via j ; (47).

186 The dyad-independent variables included panther sex (both as a node factor and node
187 mixing variable; see supplementary methods for terminology and additional variable details). We
188 assessed panther age as a categorical variable (both as a node factor and node mixing
189 variable), with subadults classified as individuals between the ages of 6 months and two years,
190 and adults classified as individuals over two years of age. We included pairwise genetic
191 relatedness from panther microsatellite data as an edge covariate. Spatial variables included a
192 node-matching variable for the location of panthers' minimum convex polygon (MCP) home
193 range centroid or capture location (hereafter *centroid*; see supplementary methods) north
194 versus south of the major I-75 freeway. In addition, we included a node covariate term for the
195 distance from the centroid to the nearest urban area (in km; USA Urban Areas layer, ArcGIS;
196 (48). Pairwise geographic distances between panthers were calculated using distances between
197 centroids (in km), and log-transformed for use as an edge covariate. Lastly, we included a
198 spatial overlap edge covariate based on the pairwise utilization distribution overlap indices of
199 95% home range kernels (49), using the *adehabitat* package in R (50).

200 Because ERGMs are prone to degeneracy with increasing complexity (46), we first
201 performed forward selection for network structural variables, followed by forward selection of
202 dyad-independent variables, while controlling for network structure. Model selection was based
203 on AIC and goodness of fit, and MCMC diagnostics were assessed for the final model
204 (supplementary methods).

205

206 *Panther population simulations*

207 To test if predictors of FIV transmission identified in the ERGM analysis can predict
208 FeLV transmission, we next simulated FeLV transmission through a network which was based
209 on these FIV predictors simulated populations representing panthers during the well-
210 characterized FeLV outbreak (2002-2004; 21). Hereafter, a *full-simulation* includes both
211 simulation of the panther population and its network of likely transmission pathways during the
212 historical outbreak period and simulation of FeLV transmission within that population. Below, we
213 describe the process for a single simulation, but these procedures were repeated for each full
214 simulation.

215 We first based the simulated population size on the range of empirical estimates from
216 2002-2004 (51). Additional characteristics of the simulated population included those identified
217 as significant variables in the ERGM analysis, which were: age category and pairwise
218 geographic distances between panther home range centroids. We randomly assigned age
219 categories to the simulated population based on the proportion of adults versus subadults. Age
220 proportions were based on age distributions in the western United States (52) which
221 qualitatively align with the historically elevated mean age of the Florida panther population (53).
222 Pairwise geographic distances for the simulated population were generated by randomly
223 assigning simulated home range centroids based on the distribution of observed centroids on
224 the landscape (supplementary methods).

225 We then used ERGM coefficients to generate network edges in the simulated panther
226 population representing potential transmission pathways between panthers. The FIV
227 transmission network spanned 15 years of observations and represents a subset of the actual
228 contact network, as it includes only those interactions that resulted in successful transmission
229 (54). We therefore had a high degree of uncertainty regarding the appropriate network density
230 for our simulations. To manage this uncertainty, we constrained density in our network
231 simulations across a range of parameter space (*net_dens*, Table 1).

232

233 **Table 1: Network and transmission simulation parameters**

Parameter	Definition	Range	Reference
Pop_size	Population size	80-120	(51)
Adult_prop	Proportion adults versus subadults	0.82-0.99	(52)
Net_dens	Simulated network density	0.05-0.15	NA
β	Probability of transmission from progressives, given effective contact	0.17-0.29	(55)
C	Constant multiplier for probability of transmission from regressives, given effective contact	0, 0.1, 0.5, 1	NA
ω	Weekly probability of contact	0.1-0.4	(56)
μ	Weekly probability of death from progressive infection	1/18, 1/26*	(21)
K	Constant multiplier for weekly probability of recovery from regressive infection	0.5, 1	NA
ν	Weekly probability of territory repopulation ("respawn rate")	1/12-1/4	NA
τ	Weekly probability of vaccination	0.5-1	NA
ve	Probability of vaccine efficacy	0.4-1	(21)
P	Proportion randomly assigned to progressive, regressive	0.25	(21)

234 *Note: Parameter gives parameter symbols or abbreviations; definition gives the description for*
 235 *each parameter. Range shows the continuous range or discrete values sampled from in*
 236 *simulations, with references giving literature supporting ranges or values. *We tested a lower*
 237 *death rate (prolonged duration of infection) due to the low number of observed panther cases*
 238 *and the generally longer infection duration in domestic cats (40).*

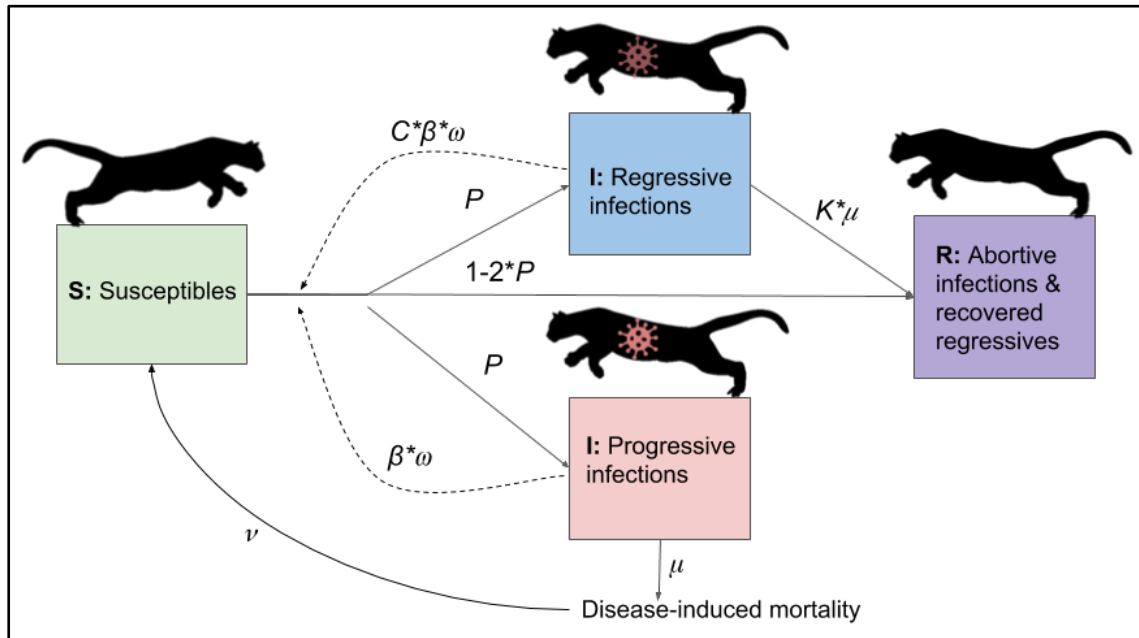
239

240 *Simulation of FeLV transmission on FIV-based networks*

241 The next step in each full simulation was to model FeLV transmission on the network
 242 generated from FIV predictors of transmission. FeLV transmission was based on a chain
 243 binomial process on the simulated networks, following a modified SIR compartmental model

244 (Figure 2). Simulations were initiated with one randomly selected infectious individual and
 245 proceeded in weekly time steps. Transmission simulations lasted until no infectious individuals
 246 remained or until 2.5 years, whichever came first.

247



248

249 **Figure 2:** Diagram of flows of individuals between compartments in transmission model. Virus
 250 icons indicate infectious states, with the regressive infection icon darkened to represent reduced
 251 or uncertain infectiousness of this class. Note: a vaccination process was also included in the
 252 transmission model, but is not shown for simplicity. With vaccination, susceptibles could be
 253 vaccinated, and vaccinated individuals subsequently infected analogously to susceptibles, but
 254 with an additional probability of $(1-v_e)$. See Table 1 for definitions of parameters.

255

256 Transmission (Figure 2) was dependent on the following: (1) existence of an edge
 257 between two individuals, (2) the dyad in question involving a susceptible and infectious
 258 individual, and (3) a random binomial draw based on the probability of transmission given
 259 contact (β , Table 1). In addition, *puma concolor* generally have low expected weekly contact

260 rates (56); we therefore included an additional weekly contact probability, represented as a
261 random binomial draw for contact in a given week (ω , Table 1).

262 Upon successful transmission, infectious individuals were randomly assigned to one of
263 three outcomes of FeLV infection (21). *Progressive* infections (probability P , Table 1) are
264 infectious, develop clinical disease, and die due to infection at a mortality rate, μ . *Regressive*
265 infections (also probability P) recover at a rate based on a constant, K , multiplied by the
266 mortality rate of progressives (Table 1). Anecdotal evidence suggests regressive individuals are
267 not infectious (21), but given ongoing uncertainty, we allowed regressives to be infectious by
268 multiplying the probability of transmission for progressives (β) by a constant, C (Table 1).
269 *Abortive* infections (probability $1-2P$) are never infectious, clearing infection and joining the
270 recovered class.

271 A vaccination process was included in simulations as panthers were vaccinated against
272 FeLV during the historical FeLV outbreak starting in 2003. Vaccination occurred at a rate, τ , and
273 applied to the whole population, as wildlife managers are unlikely to know if a panther is
274 susceptible at the time of capture or darting. However, only susceptible individuals transitioned
275 to the vaccinated class (i.e. vaccination failed in non-susceptibles). Because panthers were
276 vaccinated in the empirical outbreak with a domestic cat vaccine with unknown efficacy in
277 panthers, we allowed vaccinated individuals to become infected in transmission simulations by
278 including a binomial probability for vaccine failure (1 -vaccine efficacy, v_e , Table 1).

279 The panther population size remained roughly static through the course of the FeLV
280 outbreak (51, 57). We therefore elected not to include background mortality, but did include
281 infection-induced mortality. To maintain a consistent population size, we therefore included a
282 birth/recruitment process. Because FIV-based simulated networks drew edges based on
283 population characteristics, we treated births as a “respawning” process, in which territories
284 vacated due to mortality were reoccupied by a new susceptible at rate, ν . This approach allowed

285 us to maintain the ERGM-based network structure and is biologically reasonable, as vacated
286 panther territories are unlikely to remain unoccupied for long.

287 FeLV infection is uncommon in puma as a species, resulting in a high degree of
288 uncertainty regarding differences in within-individual infection dynamics in panthers (e.g.,
289 epidemiological parameters such as infectious period). Given these uncertainties, we performed
290 all simulations across a range of parameter space. To more efficiently cover this parameter
291 space, we generated parameter sets using a Latin hypercube design (LHS), using the lhs
292 package in R (58). We generated 150 parameter sets, conducting 50 full simulations per
293 parameter set.

294

295 *Comparison of simulation predictions to observed FeLV outbreak*

296 We compared FIV-based simulation predictions to the observed FeLV outbreak as well
297 as predictions from three simpler types of models: random networks, home range overlap-based
298 networks, and a well-mixed model. All models used the parameterizations from our LHS
299 parameter sets, as relevant.

300 For our random networks model, we generated Erdős-Rényi random networks, with the
301 simulated network densities from our LHS parameter sets (Table 1). Overlap-based networks
302 were generated using the degree distributions of panther home range overlap networks from
303 2002-2004 and simulated annealing with the R package statnet (59, 60; supplementary
304 methods). These overlap-based networks were not spatially explicit, as they were based only on
305 the degree distributions from real spatial overlap networks. For both random and overlap-based
306 networks, FeLV transmission was simulated as in the FIV-based simulations. The well-mixed
307 model was a Gillespie algorithm (stochastic, continuous time compartmental model), with rate
308 functions aligning with the chain binomial FeLV transmission probabilities (supplementary
309 methods).

310 Target ranges for predicted outcomes were based on observed FeLV dynamics (21),
311 with ranges to account for uncertainty in observations and population size in this cryptic species
312 (supplementary methods). The primary outcomes of interest were (1) duration of outbreak: 78-
313 117 weeks, (2) total number of progressive infections: 5-20, and (3) presence of spatial
314 clustering (see below). While our primary focus was progressive infections, we also included an
315 expectation that at least 5 individuals were abortive infections. Empirically, these individuals
316 were the most numerous, but as they were not clinically ill, abortive infections were less likely to
317 be detected in normal panther management; we therefore did not include an upper bound for
318 this target.

319 Using our database of qPCR results for FeLV in panthers (positive and negative tests),
320 we performed a local spatial clustering analysis of FeLV cases and controls using SaTScan
321 (50% maximum, circular window; 61), and a global cluster analysis with Cuzick and Edward's
322 test in the R package *smacpod* (1, 3, 5, 7, 9, and 11 nearest neighbors; 999 iterations; 62, 63).
323 These analyses found evidence of local (weak) and global clustering (at 3, 5, and 7
324 neighborhood levels) among progressive and regressive cases (see results, supplementary
325 methods and results). In simulations, we therefore included spatial clustering of progressive and
326 regressive cases as a target outcome.

327 For the duration of outbreaks and total number of progressives, we calculated median
328 values of both outcomes for each parameter set (i.e., 50 simulations) within each model type. If
329 a parameter set's medians were within the target ranges for both of these outcomes, it was
330 considered *feasible*. To quantify differences in model prediction performance, we fit a binomial
331 generalized linear mixed model (GLMM), assuming a logistic regression with "feasible" (vs
332 "unfeasible") as the outcome, model type as a predictor variable, and a random intercept for
333 LHS parameter set.

334 To determine if simulated results demonstrated spatial clustering, we performed
335 SaTScan spatial cluster analysis (50% maximum, circular window) and Cuzick and Edward's

336 tests (at 3, 5, and 7 nearest neighbors) on simulation results. Only FIV-based simulations were
337 spatially explicit, and we performed spatial analyses only on those parameter sets that were
338 classified as feasible. To determine if any detected clustering in FIV simulations was simply
339 based on our respawning protocol, we also performed both spatial analyses with feasible
340 overlap-based simulation results. For these, we assigned the same geographic locations to
341 nodes in the overlap-based networks from the corresponding FIV-based networks (i.e.,
342 matching simulation number from matching parameter set).

343

344 **Results**

345 *FIV transmission network analysis*

346 The main FIV network included 19 nodes (individuals) with 42 edges (representing
347 potential transmission events; network density = 0.25) after removing 9 edges that were
348 between individuals known not to be alive at the same time (Figure S1). ERGM results for the
349 main FIV network identified geometrically weighted edgewise shared partner distribution
350 (*gwesp*) and alternating k-stars (*altkstar*) as key structural variables, and age category (as a
351 node-level factor) and log transformed pairwise geographic distance as key dyad-independent
352 variables (Table 2). Though *altkstar* was not statistically significant, inclusion of this variable
353 contributed to improved AIC and goodness of fit outcomes. Adults were more likely to be
354 involved in transmission events (but see discussion of sample size limitations) and inferred
355 transmission events were more likely between individuals which were geographically closer to
356 each other. The fitted model showed reasonable goodness of fit (Figure S2). ERGM results
357 were largely consistent across two replicate analyses with alternative transmission networks
358 formed by summarizing across four single Phyloscanner outputs (see supplementary results for
359 further details).

360

361 **Table 2: Main FIV transmission network exponential random graph model results**

Variable	Estimate	SE	p-value
Edges (intercept)	-2.56	1.33	0.055
gwesp	0.98	0.26	<0.001
altkstar	-0.70	0.96	0.47
Age (Adult)	0.93	0.44	0.03
Log pairwise distance	-0.45	0.21	0.03

362 Note: “gwesp” is geometrically weighted edgewise shared partner distribution and “altkstar” is
363 alternating k-stars. Age classes were subadult and adult; pairwise distances were between
364 home range centroids. Only those variables from the final model are shown. Estimates shown
365 are untransformed; SE represents standard error; p-values less than 0.05 were considered
366 statistically significant.

367

368 FeLV simulations

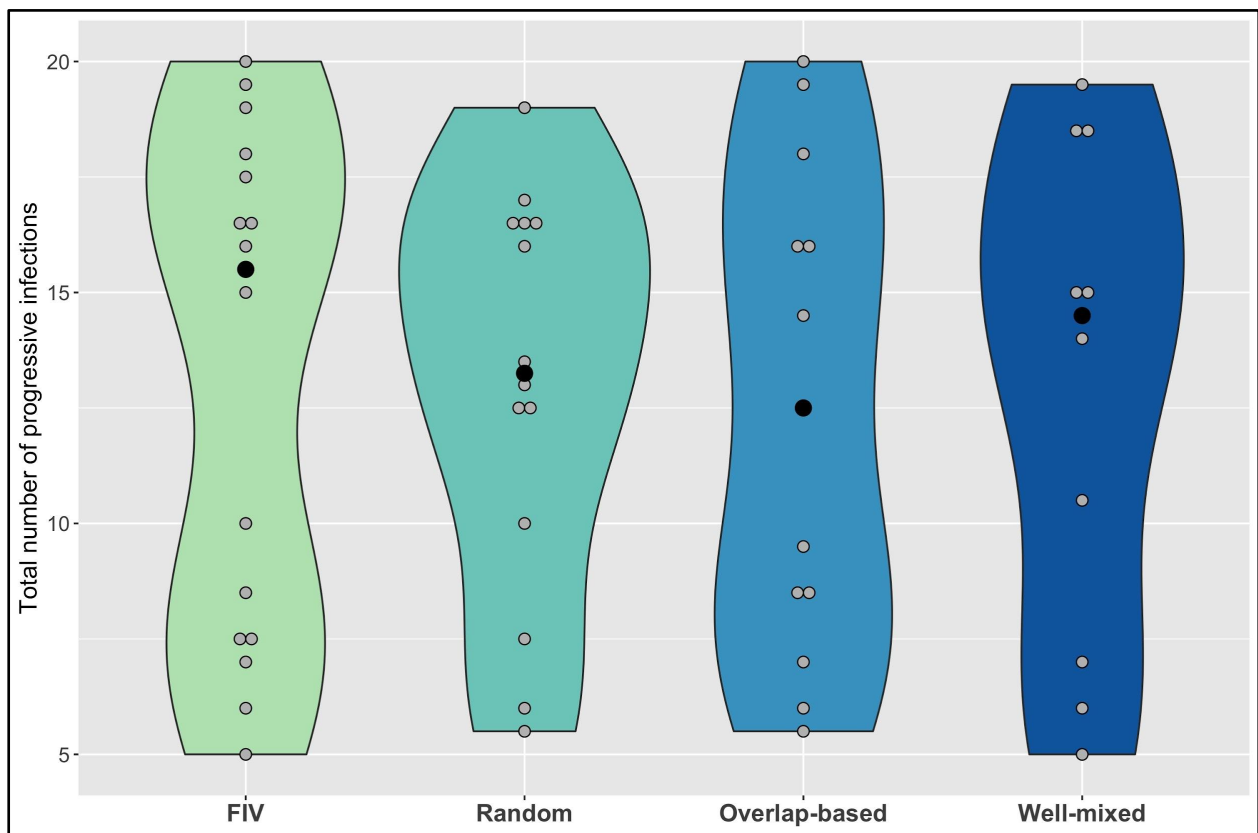
369 SaTScan analysis of observed FeLV status found weak evidence of local spatial
370 clustering (two clusters detected, but not statistically significant with $p=0.165$ and 0.997 ,
371 respectively; Figure S4). Cuzick and Edward’s tests found evidence of global clustering at 3, 5,
372 and 7 nearest neighbor levels (test statistic T_k where k is number of nearest neighbors
373 considered: $T_3 = 20$, $p = 0.049$; $T_5 = 32$, $p = 0.028$; $T_7 = 43$, $p = 0.023$). Both sets of spatial
374 analysis results were then compared against FeLV predictions from FIV and overlap-based
375 models.

376 About 9% of parameter sets across all model types were classified as feasible (Figures
377 3, S5-S6). The GLMM for model type performance (i.e., FIV-based, random, overlap-based, or
378 well-mixed) did not find statistically significant differences between odds of generating feasible
379 simulation outcomes, though the FIV-based model had the highest odds of feasibility
380 (exponentiated estimate = 1.55, though $p = 0.30$; Table S2). Feasible parameter sets from both

381 the FIV-based and overlap-based models produced some evidence of local and global spatial
382 clustering of simulated FeLV cases (Figures 4, S7). However, the FIV-based model was better
383 able to capture the size and strength (observed/expected FeLV cases) of predicted local
384 clusters (Figure 4) and was moderately better at capturing global spatial patterns (Figure S7).

385 In order to determine if certain transmission parameters were particularly important for
386 feasible performance, we performed *post hoc* random forest analyses using the R package
387 *randomForest* (64, 65) for each of the four model types (see supplementary results). While
388 random forests typically showed poor balanced accuracy and area under the curve (AUC)
389 results, the parameter shaping transmission from regressively infected individuals (C), showed
390 support for weak to moderate transmission from regressives (i.e., $C = 0.1$ or 0.5 ; Figure S10).

391



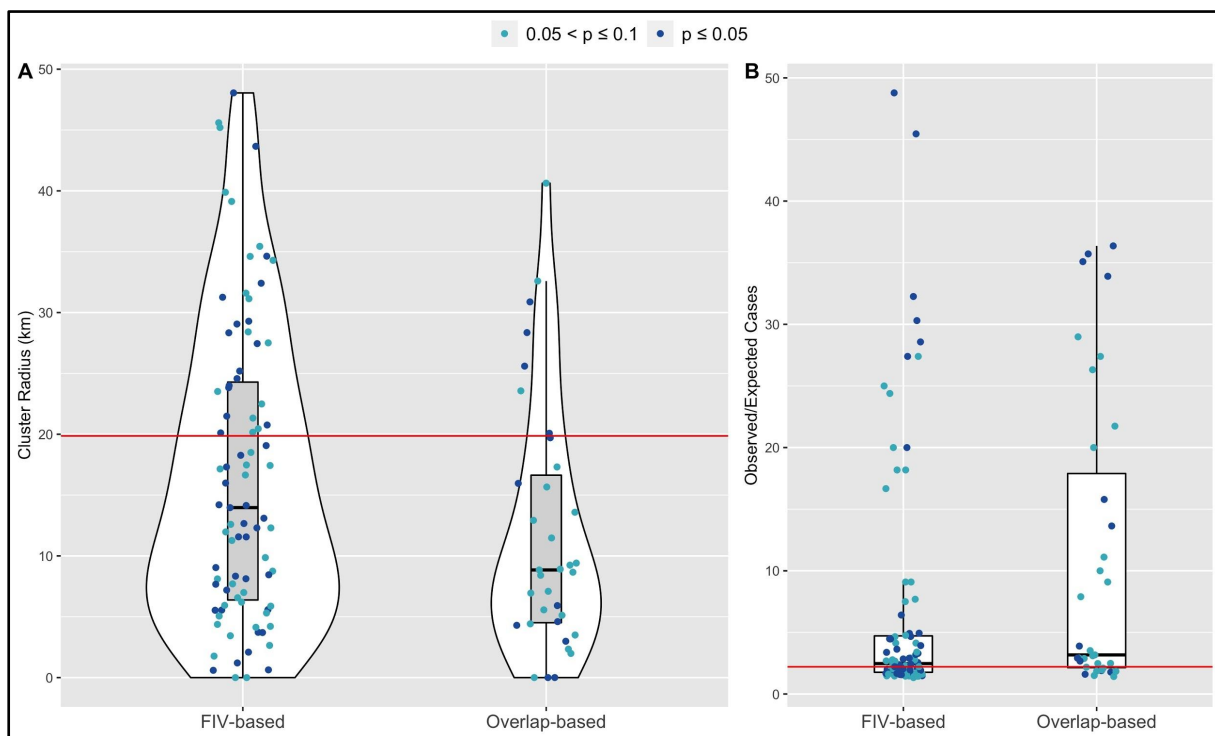
392

393 **Figure 3:** FIV-based networks perform at least as well as other models in predicting number of
394 progressive infections, as seen in violin plots of median total number of progressive infections

395 from parameter sets classified as “feasible.” To be feasible, medians needed to fall between 5
396 and 20 progressive infections, while also having median epidemic duration between 78-117
397 weeks, and a median of at least 5 abortive infections. Gray points show median values from
398 each feasible parameter set; black points are the median value within each violin plot. Model
399 types are given on the x-axis.

400

401



402

403 **Figure 4:** SaTScan cluster analysis for feasible FIV-based and overlap-based network

404 simulations show stronger agreement between empirical observations (red horizontal lines) and

405 FIV-based predictions for (A) predicted FeLV cluster size and (B) Observed/Expected FeLV

406 cases associated with the top detected cluster. Shown are feasible simulation results in which at

407 least one cluster was detected with p-value less than or equal to 0.1; further, only the results

408 from the top cluster are shown.

409

410 **Discussion**

411 In this study we develop a new approach whereby we leveraged knowledge of
412 transmission dynamics of a common apathogenic agent to prospectively predict dynamics of an
413 uncommon and virulent pathogen. Our approach was distinctly different from simpler models we
414 tested, as the apathogenic (FIV)--based approach could be used to prospectively identify
415 predictors of transmission and develop disease control plans prior to an outbreak of a virulent
416 pathogen (FeLV), while other approaches either make broad assumptions about transmission-
417 relevant contacts (e.g., homogeneous mixing), or rely on retrospective or reactive modeling. We
418 found that FIV transmission in panthers is primarily driven by distance between home range
419 centroids and age class, and that our prospective FIV-based approach predicted FeLV
420 transmission dynamics at least as well as simpler or more reactive approaches. While we do not
421 propose that this apathogenic agent approach could accurately predict exactly when, where,
422 and to whom transmission might occur, our results support the role of apathogenic agents as
423 novel tools for prospectively identifying relevant drivers of transmission and consequently
424 improving proactive disease management.

425

426 *Pairwise geographic distances and panther age class predict FIV transmission*

427 Combining genomic and network approaches, we determined that pairwise geographic
428 distances and age category structure FIV transmission in the Florida panther. Because FIV is a
429 persistent infection, we would expect cumulative risk of transmission to increase over an
430 individual's lifetime and adults would consequently be involved in more transmission events.
431 The low number of subadult individuals in our dataset, however, means that this finding must be
432 interpreted with caution.

433 Panthers are wide-ranging animals but maintain home ranges, and this appears to
434 translate to increased transmission between individuals that are close geographically. This
435 finding is further supported by the tendency for FIV phylogenies to show distinct geographic

436 clustering (66, 67), but is in contrast to other infectious agents of puma. An additional feline
437 retrovirus, feline foamy virus (FFV), does not show distinct geographic clustering but is
438 commonly transmitted between domestic cats and puma (68). A prior study of several
439 pathogens in puma across the United States rarely identified spatial autocorrelation in pathogen
440 exposures, but notably found that FIV infection status approached statistical significance
441 specifically in Florida panthers (69). The wide-ranging nature of puma appears to limit
442 geographic clustering of many infectious agents, with FIV a notable exception to this pattern.
443 Multi-host agents such as FFV are presumably more able to escape geographical limitations
444 and/or may be transmitted prior to dispersal and thereby lack spatial structuring. More generally,
445 the importance of distance rather than panther relatedness in structuring transmission may
446 support the resource dispersion or land tenure hypotheses as drivers of spatial and social
447 structuring in panthers, rather than kinship. The high inbreeding among panthers (53) may limit
448 our power for identifying a relationship between relatedness and FIV transmission, but support
449 for resource dispersion or land tenure would be in agreement with findings in other puma
450 systems (70) and even other territorial carnivores (71).

451 Surprisingly, sex was not a significant predictor of FIV transmission. FIV force of
452 infection is generally higher in male panthers, likely due to their increased fighting behaviors
453 (72). However, studies in other felid species have found mixed importance of sex for FIV
454 transmission, ranging from little to no importance (puma in the western United States: 73;
455 bobcat: 74) to importance only among certain FIV subtypes (African lions: 75). Our results add
456 to this body of research to suggest that the relationship between host sex and FIV transmission
457 is more complex than can be explained by sex-specific behaviors or susceptibility alone.

458

459 *An FIV-based model captures FeLV transmission dynamics*

460 In our study, a network model based on principles of FIV transmission produced FeLV
461 outbreak predictions consistent with the observed FeLV outbreak. The FIV-based approach

462 performed at least as well as simpler models, per our GLMM analysis, with evidence that FIV
463 better predicted the observed spatial dynamics for FeLV transmission. A key difference between
464 the FIV-based approach and other spatially-explicit methods is that FIV allowed us to determine
465 the importance of spatial dynamics prospectively and then translate to predictions of FeLV
466 transmission, rather than relying on retrospective FeLV spatial analyses. Furthermore, while
467 more complex potential drivers of transmission (e.g., host relatedness or assortative mixing by
468 age or sex) were not found to be important for FIV transmission, these may yet be key factors
469 structuring transmission in other systems. Simpler model types like random networks or
470 metapopulation models may struggle to make transmission predictions that incorporate these
471 factors as drivers of transmission-relevant contact. The predictive power we observed here
472 using an apathogenic virus could thus significantly shape proactive epidemic management
473 strategies for pathogens such as FeLV.

474 FIV and FeLV have different epidemiologies (e.g., progressive versus regressive
475 infections, duration of infectiousness); despite this, FIV-based predictors of transmission were
476 able to capture dynamics of FeLV transmission. Here, FIV determined the key drivers of close,
477 direct contact transmission in panthers, fundamentally acting as a proxy for this type of contact.
478 FeLV simulations were then able to independently account for differences in epidemiology to
479 produce appropriate predictions for a different but analogously transmitted virus. Key
480 components of this success are likely that (1) FIV is a largely species-specific virus with
481 transmission pathways closely matching intra-species transmission of FeLV, and (2) both FIV
482 and FeLV, perhaps unusually for infectious agents of puma, display spatial clustering of
483 infection. If, for example, FIV also exhibited strong vertical or environmental transmission, we
484 would no longer expect the predictive success for FeLV we observed here.

485 Domestic cats are the reservoir host for FeLV (39) and panthers are subject to repeated
486 spillover events from domestic cats (42). Determining the predictors and frequency of these
487 spillover events would be less feasible with FIV_{pco}, which adapted to the puma host (76–78).

488 Rather, targeted investigation of spillover dynamics could draw on studies of other apathogenic
489 viral candidates that are frequently transmitted from domestic cats to puma, such as FFV (68).
490 Using such agents to identify drivers of spillover events could be key for better understanding
491 the dynamics of “pathogen release from reservoir hosts” (4), which is of profound relevance
492 across wildlife, domestic animal, and human systems.

493 While few parameter sets were classified as feasible across all model types, this
494 appears to be predominantly the result of the wide range of parameter space explored through
495 our LHS sampling design. This limitation was fundamentally due to uncertainties in FeLV
496 transmission parameters, and is representative of the uncertainties experienced in predicting
497 transmission of emerging or understudied pathogens. Key here were the interacting
498 uncertainties regarding infectiousness of regressives, the number of introductions of FeLV to the
499 panther population, and the duration of FeLV infection in panthers. All three of these dynamics
500 can have significant impacts on the duration of a simulated epidemic, allowing an epidemic to
501 continue to “stutter” along at low levels (79), much as was observed in the empirical FeLV
502 outbreak. Our *post hoc* random forest analysis provided some evidence of weak transmission
503 from regressive individuals, but this finding would need to be validated with additional research,
504 as it is in stark contrast to FeLV dynamics in domestic cats. Reducing uncertainties in these
505 three key dynamics would significantly narrow the range of our predictions, and even assist in
506 ongoing management efforts for FeLV in endangered panthers.

507 Furthermore, the effect of transmission parameter uncertainties underscores the
508 importance of linking laboratory and model-based research to generate more accurate
509 transmission forecasts (80). Experimental research could help to narrow the range of parameter
510 space for FeLV—or other emerging pathogens—to produce more consistent and accurate
511 model predictions. This necessity is all the more apparent during the current COVID-19
512 pandemic, in which mathematical models have benefited from rapid laboratory and
513 epidemiological research to reduce uncertainty in model parameters.

514

515 *Limitations and future directions*

516 This study found evidence for the utility of an apathogenic agent to predict transmission
517 of a related pathogenic agent, but this approach must now be tested in additional host-pathogen
518 systems. The mixed results when using commensal agents to identify close social relationships
519 in other systems (22–27) highlights that some host-apathogenic agent combinations will work
520 better than others for determining drivers of transmission. More research is therefore necessary
521 to determine which apathogenic agents may be most suitable as markers of transmission, and
522 how divergent an apathogenic agent may be from a pathogen of interest while still predicting
523 transmission dynamics.

524 The suite of tools for inferring transmission networks from infectious agent genomes is
525 rapidly expanding (31, 81). In this study, we used the program PhyloScanner as it maximized
526 the information from our next generation sequencing viral data. However, our FIV sequences
527 were generated within a tiled amplicon framework (44, 82), which biases intrahost diversity and
528 likely limits viral haplotypes (83). PhyloScanner was originally designed to analyze RNA from
529 virions and not proviral DNA, as we have done here. We have attempted to mitigate the effects
530 of these limitations by analyzing several different PhyloScanner outputs to confirm consistency
531 in our results, and by using only binary networks to avoid putting undue emphasis on
532 transmission network edge probabilities, as these are likely highly uncertain. Further, our
533 primary conclusions from the transmission networks—that age and pairwise distance are
534 important for transmission—are biologically plausible and supported by other literature, as
535 discussed above. Nevertheless, future work should evaluate additional or alternative
536 transmission network inference platforms.

537 In addition, ERGMs assume the presence of the “full network” and it is as yet unclear
538 how missing data may affect transmission inferences (46). ERGMs are also prone to
539 degeneracy with increased complexity and do not easily capture uncertainty in transmission

540 events, as most weighted network ERGM (or generalized ERGM) approaches have been
541 tailored for count data (e.g., 84). ERGMs may therefore not be the ideal solution for identifying
542 drivers of transmission networks in all systems. Alternatives may include advancing dyad-based
543 modeling strategies (85), which may more easily manage weighted networks and instances of
544 missing data.

545 Our FIV-based approach required extensive field sampling, and many disciplines from
546 viral genomics through simulation modeling. However, with increasing availability of virome data
547 and even field-based sequencing technology, our approach may become more accessible with
548 time. Further, the predictive benefits seen here, while needing further testing and validation,
549 could become a key strategy for proactive pathogen management in species of conservation
550 concern, populations of high economic value (e.g. production animals), or populations at high
551 risk of spillover, all of which may most benefit from rapid, efficient epidemic responses.

552

553 *Conclusions*

554 Here, we integrated genomic and network approaches to identify drivers of FIV
555 transmission in the Florida panther. This apathogenic agent acted as a marker of close, direct
556 contact transmission, and was subsequently successful in predicting the observed transmission
557 dynamics of the related pathogen, FeLV. Further testing of apathogenic agents as markers of
558 transmission and their ability to predict transmission of related pathogenic agents is needed, but
559 holds great promise for revolutionizing proactive epidemic management across host-pathogen
560 systems.

561

562 **Acknowledgements**

563 Thanks to M. Michalska-Smith, K. Worsley-Tonks, J. Mistrick, and S. N. Hart for key feedback.
564 This research was supported by the National Science Foundation (DEB-1413925, 1654609, and
565 2030509). MLJG was supported by the Office of the Director, National Institutes of Health (NIH

566 T32OD010993), the University of Minnesota Informatics Institute MnDRIVE program, and the
567 Van Sloun Foundation. JLM was supported by the ACVP/STP Coalition for Veterinary Pathology
568 Fellows and the Linda Munson Fellowship for Wildlife Pathology Research. The content is solely
569 the responsibility of the authors and does not necessarily represent the official views of the
570 National Institutes of Health. Puma icon by Freepik at Flaticon.com.

571

572 **Data Availability**

573 Full R code for simulations is available on GitHub
574 (https://github.com/mjones029/FIV_FeLV_Transmission) and upon acceptance will be archived
575 at Zenodo.

576

577 **Works Cited**

- 578 1. R. M. Anderson, R. M. May, *Infectious Diseases of Humans: Dynamics and Control* (OUP
579 Oxford, 1991).
- 580 2. J. Antonovics, Transmission dynamics: critical questions and challenges. *Philos. Trans. R.
581 Soc. Lond. B Biol. Sci.* **372** (2017).
- 582 3. C. J. E. Metcalf, J. Lessler, Opportunities and challenges in modeling emerging infectious
583 diseases. *Science* **357**, 149–152 (2017).
- 584 4. R. K. Plowright, *et al.*, Pathways to zoonotic spillover. *Nat. Rev. Microbiol.* **15**, 502–510
585 (2017).
- 586 5. J. A. Drewe, Who infects whom? Social networks and tuberculosis transmission in wild
587 meerkats. *Proc. Biol. Sci.* **277**, 633–642 (2010).
- 588 6. M. Morris, M. Kretzschmar, Concurrent partnerships and transmission dynamics in
589 networks. *Soc. Networks* **17**, 299–318 (1995).
- 590 7. S. Cauchemez, *et al.*, Role of social networks in shaping disease transmission during a
591 community outbreak of 2009 H1N1 pandemic influenza. *Proc. Natl. Acad. Sci. U. S. A.* **108**,
592 2825–2830 (2011).
- 593 8. M. E. Craft, D. Caillaud, Network models: an underutilized tool in wildlife epidemiology?
594 *Interdiscip. Perspect. Infect. Dis.* **2011**, 676949 (2011).

- 595 9. M. J. Keeling, K. T. D. Eames, Networks and epidemic models. *J. R. Soc. Interface* **2**, 295–
596 307 (2005).
- 597 10. M. J. Keeling, M. E. J. Woolhouse, R. M. May, G. Davies, B. T. Grenfell, Modelling
598 vaccination strategies against foot-and-mouth disease. *Nature* **421**, 136–142 (2003).
- 599 11. D. L. Smith, B. Lucey, L. A. Waller, J. E. Childs, L. A. Real, Predicting the spatial dynamics
600 of rabies epidemics on heterogeneous landscapes. *Proc. Natl. Acad. Sci. U. S. A.* **99**,
601 3668–3672 (2002).
- 602 12. J. O. Lloyd-Smith, *et al.*, Epidemic dynamics at the human-animal interface. *Science* **326**,
603 1362–1367 (2009).
- 604 13. A. P. Dobson, *et al.*, Ecology and economics for pandemic prevention. *Science* **369**, 379–
605 381 (2020).
- 606 14. J. Pike, T. Bogich, S. Elwood, D. C. Finnoff, P. Daszak, Economic optimization of a global
607 strategy to address the pandemic threat. *Proc. Natl. Acad. Sci. U. S. A.* **111**, 18519–18523
608 (2014).
- 609 15. M. R. Keogh-Brown, R. D. Smith, The economic impact of SARS: How does the reality
610 match the predictions? *Health Policy* **88**, 110–120 (2008).
- 611 16. T. J. D. Knight-Jones, J. Rushton, The economic impacts of foot and mouth disease--What
612 are they, how big are they and where do they occur? *Prev. Vet. Med.* **112**, 161–173 (2013).
- 613 17. A. Blake, M. T. Sinclair, G. Sugiyarto, Quantifying the Impact of Foot and Mouth Disease on
614 Tourism and the UK Economy. *Tourism Econ.* **9**, 449–465 (2003).
- 615 18. C. Sillero-Zubiri, A. A. King, D. W. Macdonald, Rabies and mortality in Ethiopian wolves
616 (*Canis simensis*). *J. Wildl. Dis.* **32**, 80–86 (1996).
- 617 19. M. E. Roelke-Parker, *et al.*, A canine distemper virus epidemic in Serengeti lions (*Panthera*
618 *leo*). *Nature* **379**, 441–445 (1996).
- 619 20. E. S. Williams, E. T. Thorne, M. J. Appel, D. W. Belitsky, Canine distemper in black-footed
620 ferrets (*Mustela nigripes*) from Wyoming. *J. Wildl. Dis.* **24**, 385–398 (1988).
- 621 21. M. W. Cunningham, *et al.*, Epizootiology and management of feline leukemia virus in the
622 Florida puma. *J. Wildl. Dis.* **44**, 537–552 (2008).
- 623 22. K. L. VanderWaal, E. R. Atwill, L. A. Isbell, B. McCowan, Linking social and pathogen
624 transmission networks using microbial genetics in giraffe (*Giraffa camelopardalis*). *J. Anim.*
625 *Ecol.* **83**, 406–414 (2014).
- 626 23. A. Springer, A. Mellmann, C. Fichtel, P. M. Kappeler, Social structure and *Escherichia coli*
627 sharing in a group-living wild primate, Verreaux's sifaka. *BMC Ecol.* **16**, 6 (2016).
- 628 24. C. M. Bull, S. S. Godfrey, D. M. Gordon, Social networks and the spread of Salmonella in a
629 sleepy lizard population. *Mol. Ecol.* **21**, 4386–4392 (2012).
- 630 25. A. Blasse, *et al.*, Mother-offspring transmission and age-dependent accumulation of simian
631 foamy virus in wild chimpanzees. *J. Virol.* **87**, 5193–5204 (2013).

- 632 26. P. I. Chiyo, *et al.*, The influence of social structure, habitat, and host traits on the
633 transmission of *Escherichia coli* in wild elephants. *PLoS One* **9**, e93408 (2014).
- 634 27. M. D. J. Blyton, S. C. Banks, R. Peakall, D. M. Gordon, High temporal variability in
635 commensal *Escherichia coli* strain communities of a herbivorous marsupial. *Environ.*
636 *Microbiol.* **15**, 2162–2172 (2013).
- 637 28. S. Lax, *et al.*, Longitudinal analysis of microbial interaction between humans and the indoor
638 environment. *Science* **345**, 1048–1052 (2014).
- 639 29. S. J. Song, *et al.*, Cohabiting family members share microbiota with one another and with
640 their dogs. *Elife* **2**, e00458 (2013).
- 641 30. E. A. Archie, J. Tung, Social behavior and the microbiome. *Current Opinion in Behavioral*
642 *Sciences* **6**, 28–34 (2015).
- 643 31. M. D. Hall, M. E. J. Woolhouse, A. Rambaut, Using genomics data to reconstruct
644 transmission trees during disease outbreaks. *Rev. Sci. Tech.* **35**, 287–296 (2016).
- 645 32. M. L. J. Gilbertson, N. M. Fountain-Jones, M. E. Craft, Incorporating genomic methods into
646 contact networks to reveal new insights into animal behaviour and infectious disease
647 dynamics. *Behaviour* (2018).
- 648 33. M. D. J. Blyton, S. C. Banks, R. Peakall, D. B. Lindenmayer, D. M. Gordon, Not all types of
649 host contacts are equal when it comes to *E. coli* transmission. *Ecol. Lett.* **17**, 970–978
650 (2014).
- 651 34. B. T. Grenfell, *et al.*, Unifying the epidemiological and evolutionary dynamics of pathogens.
652 *Science* **303**, 327–332 (2004).
- 653 35. E. A. Archie, G. Luikart, V. O. Ezenwa, Infecting epidemiology with genetics: a new frontier
654 in disease ecology. *Trends Ecol. Evol.* **24**, 21–30 (2009).
- 655 36. N. M. Fountain-Jones, *et al.*, Towards an eco-phylogenetic framework for infectious disease
656 ecology. *Biol. Rev. Camb. Philos. Soc.* **93**, 950–970 (2018).
- 657 37. S. Carver, *et al.*, Pathogen exposure varies widely among sympatric populations of wild and
658 domestic felids across the United States. *Ecol. Appl.* **26**, 367–381 (2016).
- 659 38. E. Krakoff, R. B. Gagne, S. VandeWoude, S. Carver, Variation in Intra-individual Lentiviral
660 Evolution Rates: a Systematic Review of Human, Nonhuman Primate, and Felid Species. *J.*
661 *Viol.* **93** (2019).
- 662 39. M. A. Brown, *et al.*, Genetic characterization of feline leukemia virus from Florida panthers.
663 *Emerg. Infect. Dis.* **14**, 252–259 (2008).
- 664 40. K. Hartmann, Clinical aspects of feline retroviruses: a review. *Viruses* **4**, 2684–2710 (2012).
- 665 41. C. E. Greene, *Infectious diseases of the dog and cat*, 4th ed.. (Elsevier/Saunders, 2012).
- 666 42. E. S. Chiu, *et al.*, Multiple Introductions of Domestic Cat Feline Leukemia Virus in
667 Endangered Florida Panthers. *Emerg. Infect. Dis.* **25**, 92–101 (2019).

- 668 43. M. Van De Kerk, D. P. Onorato, J. A. Hostetler, B. M. Bolker, M. K. Oli, Dynamics,
669 persistence, and genetic management of the endangered florida panther population.
670 *Wildlife Monogr.* **203**, 3–35 (2019).
- 671 44. J. L. Malmberg, *et al.*, Altered lentiviral infection dynamics follow genetic rescue of the
672 Florida panther. *Proc. Biol. Sci.* **286**, 20191689 (2019).
- 673 45. C. Wymant, *et al.*, PHYLOSCANNER: Inferring Transmission from Within- and Between-
674 Host Pathogen Genetic Diversity. *Mol. Biol. Evol.* **35**, 719–733 (2018).
- 675 46. M. J. Silk, D. N. Fisher, Understanding animal social structure: exponential random graph
676 models in animal behaviour research. *Anim. Behav.* **132**, 137–146 (2017).
- 677 47. M. Morris, M. S. Handcock, D. R. Hunter, Specification of Exponential-Family Random
678 Graph Models: Terms and Computational Aspects. *J. Stat. Softw.* **24**, 1548–7660 (2008).
- 679 48. Esri, National Atlas of the United States, United States Geological Survey, Department of
680 Commerce, Census Bureau-Geography Division, USA Urban Areas (FeatureServer).
- 681 49. J. Fieberg, C. O. Kochanny, Lanham, Quantifying home-range overlap: the importance of
682 the utilization distribution. *J. Wildl. Manage.* **69**, 1346–1359 (2005).
- 683 50. C. Calenge, The package adehabitat for the R software: tool for the analysis of space and
684 habitat use by animals. *Ecological Modelling* **197**, 1035 (2006).
- 685 51. B. T. McClintock, D. P. Onorato, J. Martin, Endangered Florida panther population size
686 determined from public reports of motor vehicle collision mortalities. *J. Appl. Ecol.* **52**, 893–
687 901 (2015).
- 688 52. K. A. Logan, L. L. Sweanor, *Desert Puma: Evolutionary Ecology And Conservation Of An*
689 *Enduring Carnivore* (Island Press, 2001).
- 690 53. W. E. Johnson, *et al.*, Genetic restoration of the Florida panther. *Science* **329**, 1641–1645
691 (2010).
- 692 54. M. E. Craft, Infectious disease transmission and contact networks in wildlife and livestock.
693 *Philos. Trans. R. Soc. Lond. B Biol. Sci.* **370** (2015).
- 694 55. E. Fromont, M. Artois, M. Langlais, F. Courchamp, D. Pontier, Modelling the feline leukemia
695 virus (FeLV) in natural populations of cats (*Felis catus*). *Theor. Popul. Biol.* **52**, 60–70
696 (1997).
- 697 56. L. M. Elbroch, H. Quigley, Social interactions in a solitary carnivore. *Curr. Zool.* **63**, 357–
698 362 (2016).
- 699 57. R. T. McBride, R. T. McBride, R. M. McBride, C. E. McBride, Counting Pumas by
700 Categorizing Physical Evidence. *Southeast. Nat.* **7**, 381–400 (2008).
- 701 58. R. Carnell, lhs: Latin hypercube samples. *R package version 0.10*, URL [http://CRAN.R-](http://CRAN.R-project.org/package=lhs)
702 [project.org/package=lhs](http://CRAN.R-project.org/package=lhs) (2012).
- 703 59. M. S. Handcock, D. R. Hunter, C. T. Butts, S. M. Goodreau, M. Morris, statnet: Software
704 tools for the representation, visualization, analysis and simulation of network data. *J. Stat.*

- 705 *Softw.* **24**, 1548 (2008).
- 706 60. J. J. H. Reynolds, B. T. Hirsch, S. D. Gehrt, M. E. Craft, Raccoon contact networks predict
707 seasonal susceptibility to rabies outbreaks and limitations of vaccination. *J. Anim. Ecol.* **84**,
708 1720–1731 (2015).
- 709 61. M. Kulldorff, A spatial scan statistic. *Communications in Statistics - Theory and Methods* **26**,
710 1481–1496 (1997).
- 711 62. J. French, smacpod: Statistical Methods for the Analysis of Case-Control Point Data (2020).
- 712 63. J. Cuzick, R. Edwards, Spatial clustering for inhomogeneous populations. *J. R. Stat. Soc.*
713 **52**, 73–96 (1990).
- 714 64. A. Liaw, M. Wiener, Classification and Regression by randomForest. *R News* **2**, 18–22
715 (2002).
- 716 65. L. A. White, S. VandeWoude, M. E. Craft, A mechanistic, stigmergy model of territory
717 formation in solitary animals: Territorial behavior can dampen disease prevalence but
718 increase persistence. *PLoS Comput. Biol.* **16**, e1007457 (2020).
- 719 66. J. S. Lee, *et al.*, Evolution of puma lentivirus in bobcats (*Lynx rufus*) and mountain lions
720 (*Puma concolor*) in North America. *J. Virol.* **88**, 7727–7737 (2014).
- 721 67. S. P. Franklin, *et al.*, Frequent transmission of immunodeficiency viruses among bobcats
722 and pumas. *J. Virol.* **81**, 10961–10969 (2007).
- 723 68. S. Kraberger, *et al.*, Frequent cross-species transmissions of foamy virus between
724 domestic and wild felids. *Virus Evol* **6**, vez058 (2020).
- 725 69. M. L. J. Gilbertson, S. Carver, S. VandeWoude, Is pathogen exposure spatially
726 autocorrelated? Patterns of pathogens in puma (*Puma concolor*) and bobcat (*Lynx rufus*)
727 (2016).
- 728 70. L. M. Elbroch, P. E. Lendrum, H. Quigley, A. Caragiulo, Spatial overlap in a solitary
729 carnivore: support for the land tenure, kinship or resource dispersion hypotheses? *J. Anim.*
730 *Ecol.* **85**, 487–496 (2016).
- 731 71. E. E. Brandell, *et al.*, Group density, disease, and season shape territory size and overlap
732 of social carnivores. *J. Anim. Ecol.* (2020) <https://doi.org/10.1111/1365-2656.13294>.
- 733 72. J. J. H. Reynolds, *et al.*, Feline immunodeficiency virus in puma: Estimation of force of
734 infection reveals insights into transmission. *Ecol. Evol.* **9**, 11010–11024 (2019).
- 735 73. N. M. Fountain-Jones, *et al.*, Host relatedness and landscape connectivity shape pathogen
736 spread in a large secretive carnivore. *bioRxiv*, 816009 (2019).
- 737 74. N. M. Fountain-Jones, *et al.*, Urban landscapes can change virus gene flow and evolution
738 in a fragmentation-sensitive carnivore. *Mol. Ecol.* **26**, 6487–6498 (2017).
- 739 75. N. M. Fountain-Jones, *et al.*, Linking social and spatial networks to viral community
740 phylogenetics reveals subtype-specific transmission dynamics in African lions. *J. Anim.*
741 *Ecol.* **86**, 1469–1482 (2017).

- 742 76. D. M. Lagana, *et al.*, Characterization of regionally associated feline immunodeficiency
743 virus (FIV) in bobcats (*Lynx rufus*). *J. Wildl. Dis.* **49**, 718–722 (2013).
- 744 77. S. VandeWoude, C. Apetrei, Going wild: lessons from naturally occurring T-lymphotropic
745 lentiviruses. *Clin. Microbiol. Rev.* **19**, 728–762 (2006).
- 746 78. S. VandeWoude, J. Troyer, M. Poss, Restrictions to cross-species transmission of lentiviral
747 infection gleaned from studies of FIV. *Vet. Immunol. Immunopathol.* **134**, 25–32 (2010).
- 748 79. S. Blumberg, J. O. Lloyd-Smith, Inference of $R(0)$ and transmission heterogeneity from the
749 size distribution of stuttering chains. *PLoS Comput. Biol.* **9**, e1002993 (2013).
- 750 80. R. K. Plowright, S. H. Sokolow, M. E. Gorman, P. Daszak, J. E. Foley, Causal inference in
751 disease ecology: investigating ecological drivers of disease emergence. *Front. Ecol.*
752 *Environ.* **6**, 420–429 (2008).
- 753 81. S. M. Firestone, *et al.*, Reconstructing foot-and-mouth disease outbreaks: a methods
754 comparison of transmission network models. *Sci. Rep.* **9**, 4809 (2019).
- 755 82. J. Quick, *et al.*, Multiplex PCR method for MinION and Illumina sequencing of Zika and
756 other virus genomes directly from clinical samples. *Nat. Protoc.* **12**, 1261–1276 (2017).
- 757 83. N. D. Grubaugh, *et al.*, An amplicon-based sequencing framework for accurately measuring
758 intrahost virus diversity using PrimalSeq and iVar. *Genome Biol.* **20**, 8 (2019).
- 759 84. P. N. Krivitsky, Exponential-family random graph models for valued networks. *Electron. J.*
760 *Stat.* **6**, 1100–1128 (2012).
- 761 85. A. Yang, *et al.*, Effects of Social Structure and Management on Risk of Disease
762 Establishment in Wild Pigs. *J. Anim. Ecol.* (2020) <https://doi.org/10.1111/1365-2656.13412>.
- 763